International Journal of Mechanical and Electrical Engineering
ISSN: 3005-9615 (Print), ISSN: 3005-7132 (Online) | Volume 5, Number 3, Year 2025
DOI: https://doi.org/10.62051/ijmee.v5n3.05
Journal homepage: https://wepub.org/index.php/IJMEE/index

Analysis of the Influence of Arc Transition Oil Cavity Structure on the Performance of High-Speed Gear Hobbing Machine Hydrostatic Spindle

Jinyu Li

Tianjin University of Technology and Education, Tianjin, China

ABSTRACT

This study investigates the influence of arc transition oil cavity structure on the load-bearing characteristics of hydrostatic oil films in high-speed gear hobbing machine spindles under high-stroke conditions. By establishing fluid simulation models of oil cavity structures with different arc radii (r=0.5, 1.0, 1.5, and 2.0 mm), the effects of parameters such as eccentricity and stroke speed on oil film pressure and shear force distribution were systematically analyzed. The results demonstrate that the arc transition oil cavity structure significantly enhances the load-bearing capacity and lubrication performance of the hydrostatic oil film. Specifically, the structure with an arc radius of r=2.0 mm exhibits the most uniform pressure distribution, the lowest maximum pressure and shear force, and optimal performance. While eccentricity has a minor impact on pressure distribution, increasing eccentricity raises pressure on the eccentric side and slightly reduces it on the opposite side. At an eccentricity of 0.5, slight shear force concentration occurs on the eccentric side. Under high stroke speeds (1.0–2.0 m/s), both oil film pressure and shear force increase with speed, but the r=2.0 mm cavity structure remains the most stable, with no significant expansion of shear force concentration zones. Optimizing the oil cavity structure and employing higher supply pressure effectively improves the lubrication performance and operational stability of the hydrostatic spindle, providing theoretical and practical guidance for the design of high-speed gear hobbing machine spindles.

KEYWORDS

Transition Oil Cavity Structure; Hydrostatic Spindle; Oil Film load-bearing Characteristics; High-speed gear Hobbing Machine.

1. INTRODUCTION

In practical operating conditions, in addition to production parameters such as stroke speed, oil supply pressure, and eccentricity, the structural parameters of hydrostatic spindles and bushings also significantly affect the performance of high-speed gear hobbing machine hydrostatic spindles. Consequently, optimizing process parameters to enhance spindle performance under identical working conditions has become a key research focus in recent years. Scholars worldwide have conducted in-depth investigations on this subject.

For hydrostatic thrust bearings under rotational conditions about the axis, Yu et al. [1][2][3] examined the influence of pressure-equalizing groove structures on the performance of aerostatic thrust bearings. Numerical calculations and experimental comparisons demonstrated that incorporating pressure-equalizing grooves significantly improves bearing performance. Shao et al. [1] investigated the effect of circular oil cavities in fluid-lubricated hydrostatic thrust bearings. Experimental results indicated that in large hydrostatic thrust bearings, shallow oil cavities outperform deep ones due to

Content from this work may be used under the terms of CC BY-NC 4.0 licence (https://creativecommons.org/licenses/by-nc/4.0/).
Published by Warwick Evans Publishing.

hydrodynamic effects. Li et al. [4] explored different gas slit configurations and gas film thicknesses in CO_2-based aerostatic thrust bearings. Kumar et al. [5] studied various oil cavity shapes, revealing that optimal geometric design and restrictor selection are crucial for bearing performance. Kodnyanko et al. [6][7] developed a membrane-type displacement compensator for hydrostatic thrust bearings, proving its effectiveness in enhancing machining accuracy. Liu et al. [8] simulated radial pressure-equalizing grooves of different dimensions, finding groove depth substantially affects load capacity while width has minimal impact, providing valuable design guidelines.

For radial hydrostatic bearings under high-speed rotation, Wang et al. [9]proposed micro-textures to improve lubrication, experimentally verifying that strategic texture patterns significantly boost bearing performance while offering practical applications for industrial micro-surface engineering. Tauviqirrahman et al. [10] investigated texture depth effects considering cavitation, revealing decreased load capacity with increased depth and identifying an optimal depth for peak lubrication efficiency.

For linear reciprocating motion in hydrostatic guides, Fritz et al. [11] designed a novel micro-clearance hydrostatic guide, verifying via experiments that the structure reduces flow loss and machine tool resonance frequency, showing strong potential for high-speed machining applications. Wang et al. [12] developed a dual-slit oil cavity design that effectively suppresses vortex formation, with slit width critically influencing stability in ultra-precision machines.

These studies demonstrate significant progress in optimizing structural parameters for hydrostatic thrust bearings, high-speed radial bearings, and linear guides. However, high-speed gear hobbing machine hydrostatic spindles operate under complex conditions combining rapid reciprocating strokes with slow rotation—far exceeding conventional linear guide speeds—while existing parameter optimization research remains limited. Therefore, structural parameter optimization for these spindles holds substantial academic and engineering value for improving machining quality and extending service life.

2. BOUNDARY CONDITIONS OF HYDROSTATIC OIL FILM

2.1. Flow Regime of Hydrostatic Oil Film

The hydrostatic spindle, bushing, and oil film models studied in this paper are illustrated in Figure 1.

(a) Hydrostatic spindle (b) Hydrostatic bushing (c) Hydrostatic oil film

Figure 1. Research models in this study

2.2. Page Numbers

This study employs the Reynolds number (Re) as the criterion for determining the flow regime type of the hydrostatic oil film. According to fluid mechanics theory, the flow state can be classified by comparing the Reynolds number with its critical value (Recr). When the Reynolds number is below

the critical value, the flow exhibits laminar characteristics; when it exceeds the critical value, the flow transitions to turbulent. The Reynolds number is calculated as follows:

$$Re_{cr} = \frac{Q_{cr}}{2\pi dv\prime} \tag{1}$$

$$Q_{cr} = \frac{\pi dph_0^2}{12\mu l} \tag{2}$$

2.3. Hydrostatic Oil Film Thickness Equation

Under actual operating conditions, the high-speed gear hobbing machine's hydrostatic spindle develops varying degrees of eccentricity due to different radial loads, as illustrated in Figure 2.

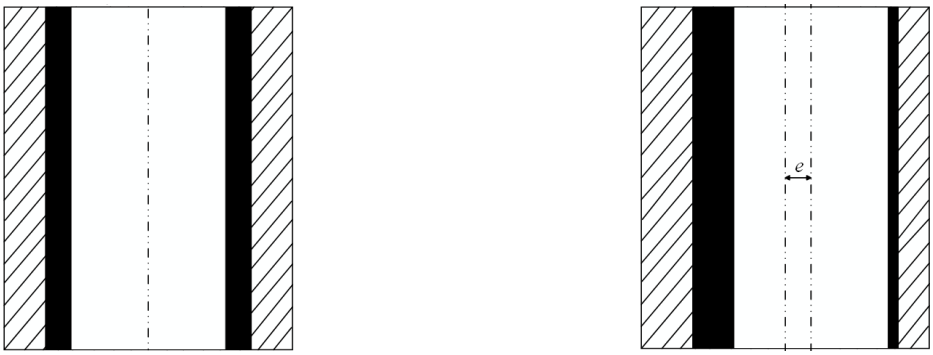

(a) Unloaded condition (b) Loaded eccentric condition

Figure 2. Schematic diagram of eccentricity states in hydrostatic spindle:

When the hydrostatic spindle is free from radial loads, the initial hydrostatic oil film thickness is given by:

$$h = (d_2 - d_1)/2 \tag{3}$$

The minimum oil film thickness h_0 under eccentric loading conditions of the hydrostatic spindle is expressed as:

$$h_0 = h(1 + \varepsilon cos\theta) \tag{4}$$

3. EFFECTS OF STRUCTURAL PARAMETERS ON LOAD-BEARING CHARACTERISTICS OF HYDROSTATIC OIL FILMS WITH DIFFERENT ARC TRANSITION CAVITY RADII

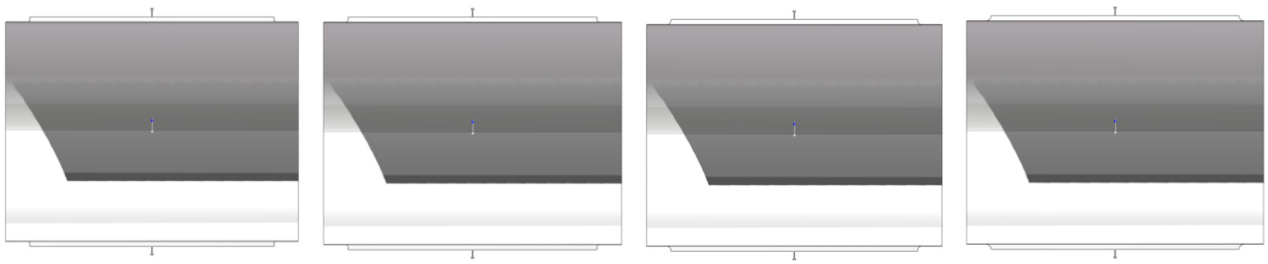

(a) r=0.5mm (b) r=1.0mm (c) r=1.5mm (d) r=2.0mm

Figure 3. Cross-sectional views of oil film profiles in linear transition cavity structures with different angles

To analyze the influence of different arc radii on the load-bearing characteristics of oil films in arc transition cavity structures and identify optimal geometric parameters, this section establishes four fluid simulation models with transition radii of r=0.5, 1.0, 1.5, and 2.0 mm.

To investigate the effects of eccentricity on the load-bearing characteristics of hydrostatic oil films in linear transition cavity structures with different angles (60°, 45°, and 30°), the pressure distribution contours are systematically analyzed in Figures 4, 5, 6and7, respectively.

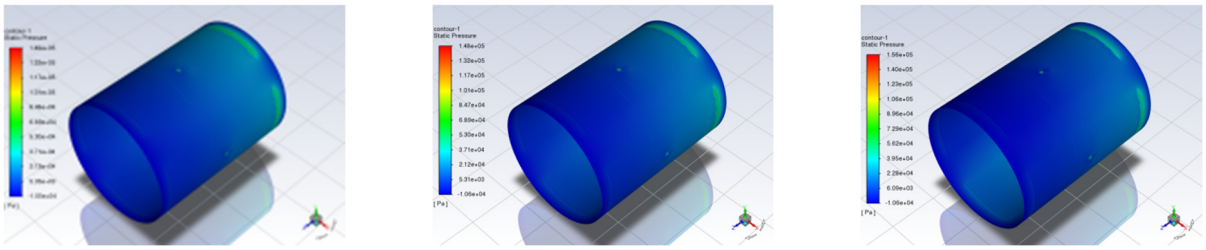

(a) ε=0.0 (b) ε=0.1 (c) ε=0.2

(d) ε=0.3 (e) ε=0.4 (f) ε=0.5

Figure 4. Pressure Contour Maps of Oil Film in 0.5 mm Radius Arc Transition Cavity Structure under Different Eccentricity Ratios

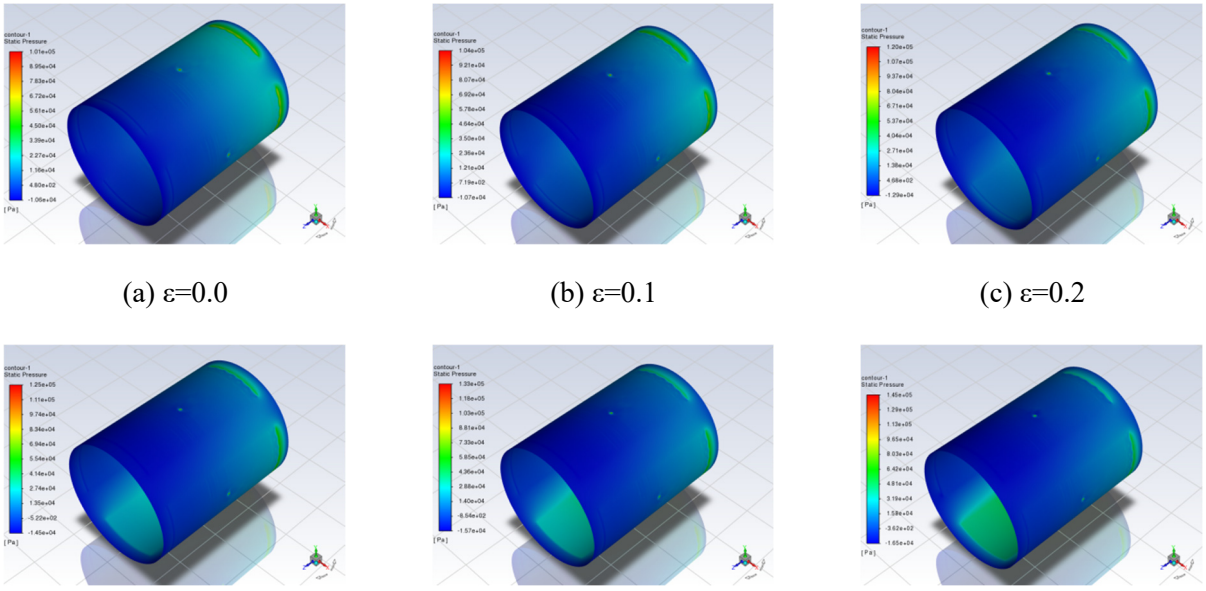

(a) ε=0.0 (b) ε=0.1 (c) ε=0.2

(d) ε=0.3 (e) ε=0.4 (f) ε=0.5

Figure 5. Pressure Contour Maps of Oil Film in 1.0 mm Radius Arc Transition Cavity Structure under Varying Eccentricity Conditions

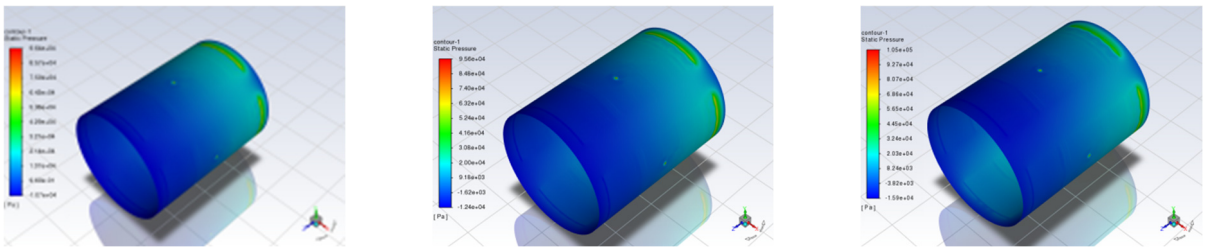

(a) ε=0.0 (b) ε=0.1 (c) ε=0.2

(d) ε=0.3 (e) ε=0.4 (f) ε=0.5

Figure 6. Pressure nephogram of oil film in r=1.5 arc transition cavity structure under different eccentricity ratios

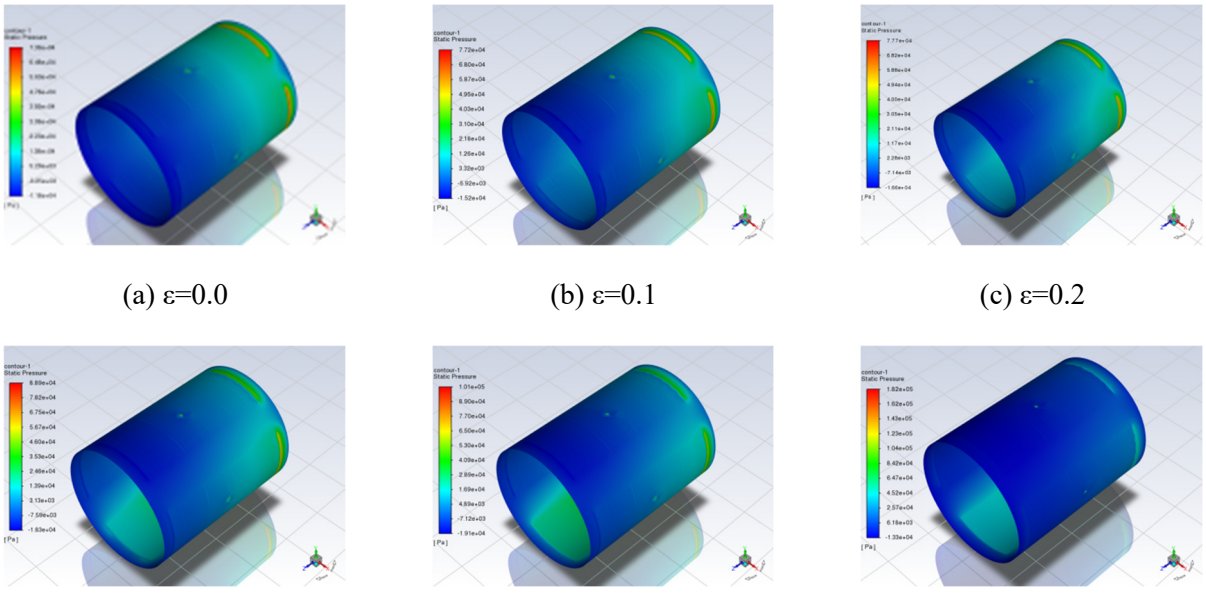

(a) ε=0.0 (b) ε=0.1 (c) ε=0.2

(d) ε=0.3 (e) ε=0.4 (f) ε=0.5

Figure 7. Pressure nephogram of oil film in r=2.0 arc transition cavity structure under different eccentricity ratios

As shown in Figures 4 to 7, variations in eccentricity do not significantly affect the pressure distribution of the hydrostatic oil film in arc transition cavity structures.

The variation trends of the maximum oil film pressure for straight transition cavity structures with different angles under various eccentricity ratios are summarized in Figure 8.

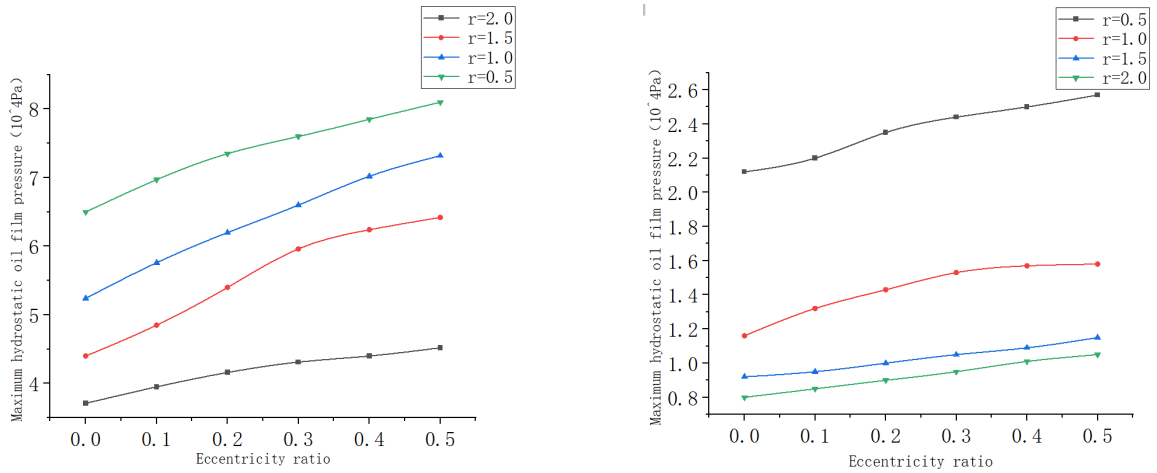

(a) Maximum pressure on eccentric side for different oil cavity structures

(b) Maximum pressure on opposite-eccentric side for different oil cavity structures

Figure 8. Variation trend of maximum oil film pressure in arc transition cavities with different radii under various eccentricity ratios

As shown in Figure 8, as the eccentricity increases, the maximum pressure of the oil film with different arc transition cavity radii exhibits a rising trend, though the increase is relatively small. On both the eccentric side and the opposite side, the hydrostatic oil film with an arc radius of r = 2.0 mm produces the lowest maximum pressure.

To investigate the influence of eccentricity on the shear force distribution of oil films with different arc transition cavity radii, the shear force contour maps for four transition cavity types (r = 0.5, 1.0, 1.5, and 2.0 mm) under varying eccentricity ratios are summarized in Figures 9 to 12. The results indicate that changes in eccentricity have little impact on the shear force distribution of the oil film across different arc transition cavity structures.

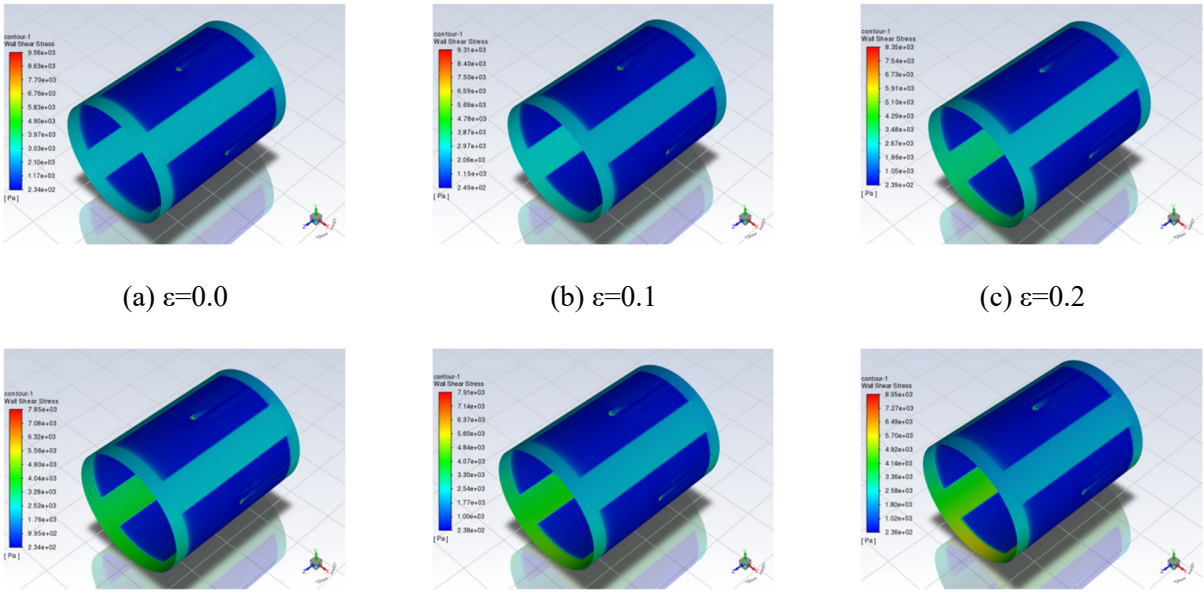

(a) ε=0.0 (b) ε=0.1 (c) ε=0.2

(d) ε=0.3 (e) ε=0.4 (f) ε=0.5

Figure 9. Shear stress nephogram of oil film in r=0.5 arc transition cavity under different eccentricity ratios

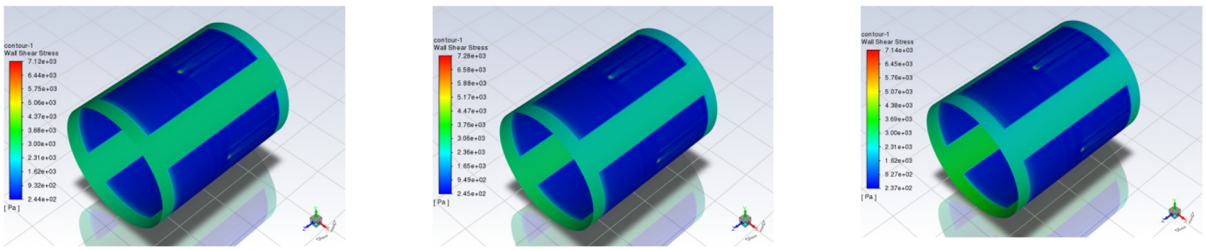

(a) ε=0.0 (b) ε=0.1 (c) ε=0.2

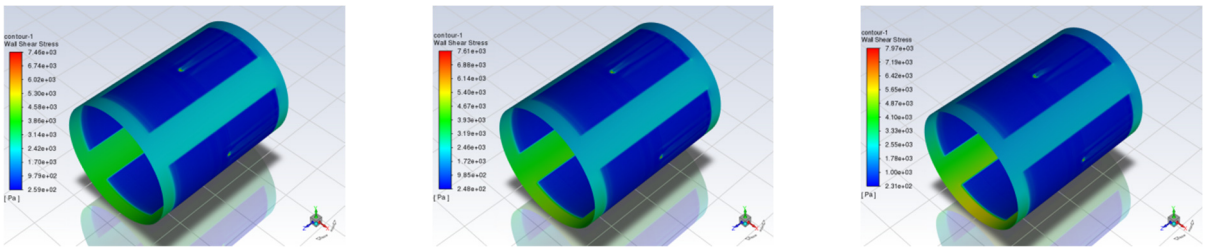

(d) ε=0.3 (e) ε=0.4 (f) ε=0.5

Figure 10. Shear stress nephogram of oil film in r=1.0 arc transition cavity under different eccentricity ratios

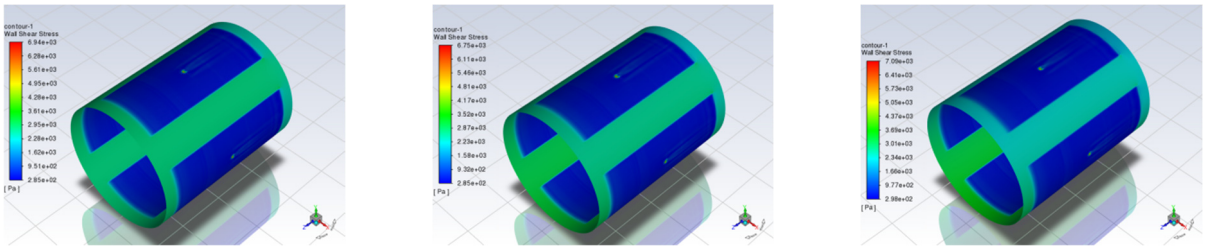

(a) ε=0.0 (b) ε=0.1 (c) ε=0.2

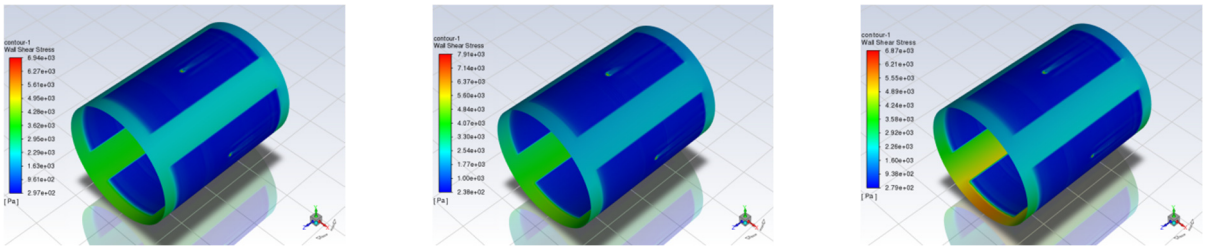

(d) ε=0.3 (e) ε=0.4 (f) ε=0.5

Figure 11. Shear stress nephogram of oil film in r=1.5 arc transition cavity under different eccentricity ratios

The variation trends of the maximum oil film pressure on both the eccentric side and the opposite side of the hydrostatic oil film with different arc transition cavity radii under various eccentricity ratios are summarized in Figure 13.

As shown in Figure 13(a), the maximum pressure on the eccentric side generally increases with the rise in eccentricity. Among the tested configurations, the arc transition cavity with a radius of r = 2.0 mm produces the minimum maximum shear force in the hydrostatic oil film.

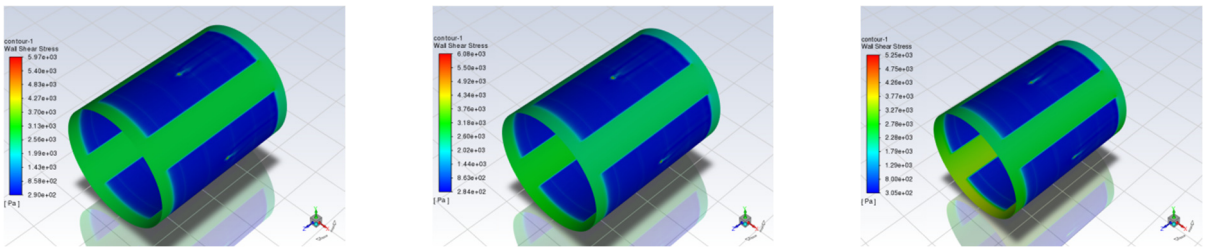

(a) ε=0.0 (b) ε=0.1 (c) ε=0.2

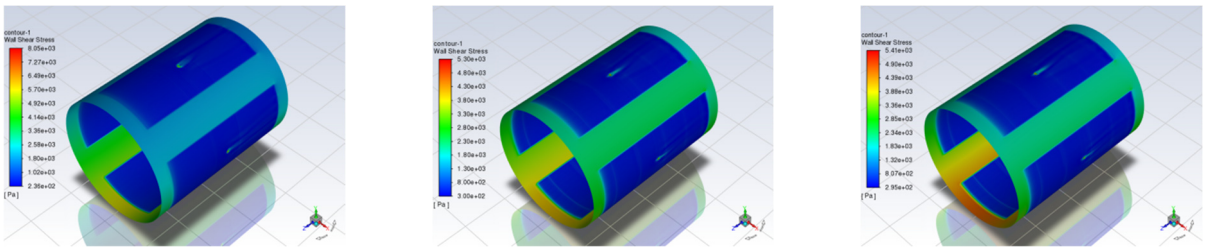

(d) ε=0.3 (e) ε=0.4 (f) ε=0.5

Figure 12. Shear stress nephogram of oil film in r=2.0 arc transition cavity under different eccentricity ratios

Figure 13(b) reveals that as the eccentricity increases, the maximum pressure on the opposite side of the eccentricity gradually decreases for all arc transition cavity radii, though the reduction is relatively slight.

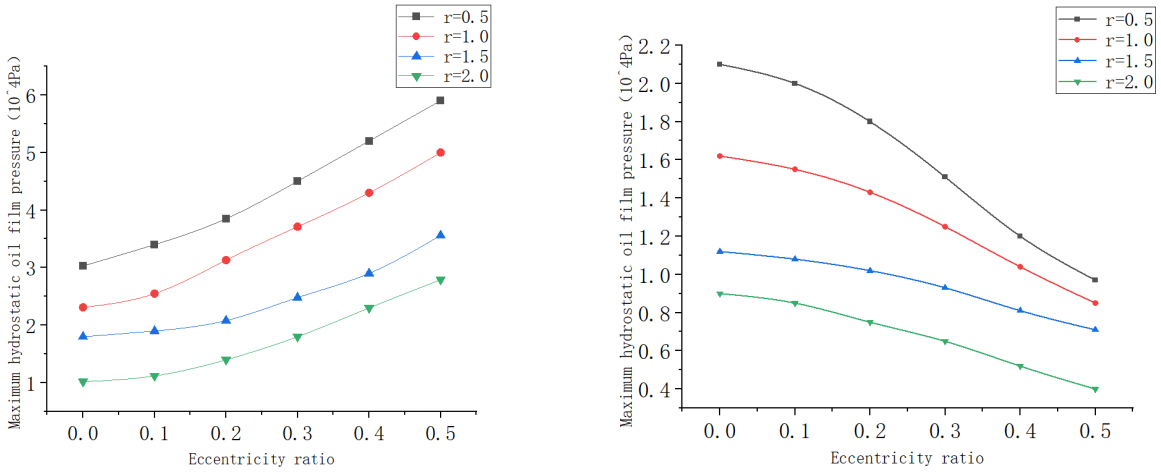

(a) Maximum shear force on the eccentric side of the oil film for different oil cavity structures

(b) Maximum shear force on the opposite side of the eccentricity for different oil cavity structures

Figure 13. Variation trend of the maximum shear force of the oil film with different arc transition oil cavity radii under various eccentricity ratios

4. SUMMARY

This chapter established a fluid simulation model for hydrostatic oil films with arc transition oil cavity structures of different geometric parameters. It systematically investigated the influence of eccentricity and stroke speed on the pressure and shear force of the hydrostatic oil film, and further explored the optimal structural parameters for the hydrostatic spindle of a gear shaping machine under the same working conditions. The results show that, compared to the structure without a transition oil

cavity, adopting a transition oil cavity structure can significantly improve the load-bearing characteristics and lubrication performance of the hydrostatic oil film. When an arc transition oil cavity structure is selected, the oil film exhibits the most optimal working performance at an arc radius of r = 2.0 mm. Additionally, to maintain the stability of the hydrostatic oil film under the reciprocating motion of the spindle, a higher supply oil pressure should be selected within a reasonable range. Finally, experimental verification confirmed that the lubrication performance of the hydrostatic spindle system with a transition oil cavity structure can be improved to a certain extent.

CONFLICTS OF INTEREST

The authors declare that they have no conflict of interest.

ACKNOWLEDGMENTS

This is the place to fill in information about funds, sponsors, etc. that need to be thanked.

REFERENCES

[1] Shao J, Liu G, Yu X, et al. Effect of Recess Depth on Lubrication Performance of Annular Recess Hydrostatic Thrust Bearing by Constant Rate Flow[J]. Industrial Lubrication and Tribology, 2018, 70(1): 68-75..

[2] Yu M, Yu X, Zheng X, et al. Influence of Recess Shape on Comprehensive Lubrication Performance of High Speed and Heavy Load Hydrostatic Thrust Bearing[J]. Industrial Lubrication and Tribology, 2018, 71(2): 301-308.

[3] Yu X, Zhang R, Zhou D, et al. Effects of Oil Recess Structural Parameters on Comprehensive Tribological Properties in Multi-pad Hydrostatic Thrust Bearing for CNC Vertical Processing Equipment Based on Low Power Consumption[J]. Energy Reports, 2021, 7: 8258-8264.

[4] Li L, Xie Y. Effect of Operating Condition and Structural Parameter in the Hydrostatic Thrust CO 2 Bearing[J]. Journal of Thermal Science, 2019, 28: 454-462.

[5] Kumar V, Sharma S C. Magneto-hydrostatic Lubrication of Thrust Bearings Considering Different Configurations of Recess[J]. Industrial Lubrication and Tribology, 2019, 71(7): 915-923.

[6] Kodnyanko V A, KurzakoV A S. Static Characteristics of a Hydrostatic Thrust Bearing with a Membrane Displacement Compensator[J]. FME Transactions, 2021, 49(3): 764-768.

[7] Kodnyanko V, KurzakoV A, GrigorieVa O, et al. Theoretical Disquisition on the Static and Dynamic Characteristics of an Adaptive Stepped Hydrostatic Thrust Bearing with a Displacement Compensator[J]. Mathematics, 2021, 9(22): 2949.

[8] Liu Y, Cao Z, Zhang Y, et al. Design and Research of Symmetrical Multi-throttle Thrust Hydrostatic Bearing Based on Comparative Analysis of Various Meshes[J]. Symmetry, 2022, 14(2): 351.

[9] Wang L, Zhang W, Zhao X, et al. Optimization Lubrication Performance of Journal Bearings with Microtexture[J]. Industrial Lubrication and Tribology, 2022, 74(6): 619-628.

[10] TauViqirrahman M, Jamari J, Muchammad M, et al. Hydrodynamic Lubrication Analysis of Hydrophobic Textured Journal Bearing Considering Cavitation[J]. Cogent Engineering, 2022, 9(1): 2069997.

[11] Fritz M, Groeb M. Increasing Performance and Energy Efficiency of a Machine Tool through Hydrostatic Linear Guideways with Single Digit Micrometer Fluid Film Thickness[J]. MM Science Journal, 2021, 2021: 5241-5246.

[12] Wang Y, Wu H, Rong Y. Analysis of Hydrostatic Bearings Based on a Unstructured Meshing Scheme and Turbulence Model[J]. Machines, 2022, 10(11): 1072.